© 2016. Published by The Company of Biologists Ltd | Journal of Experimental Biology (2016) 219, 887-896 doi:10.1242/jeb.134502

RESEARCH ARTICLE

The role of an ancestral hyperpolarization-activated cyclic nucleotide-gated K^+ channel in branchial acid-base regulation in the green crab, *Carcinus maenas*

Sandra Fehsenfeld[1,2,*] and Dirk Weihrauch[2]

ABSTRACT

Numerous electrophysiological studies on branchial K^+ transport in brachyuran crabs have established an important role for potassium channels in osmoregulatory ion uptake and ammonia excretion in the gill epithelium of decapod crustaceans. However, hardly anything is known of the actual nature of these channels in crustaceans. In the present study, the identification of a hyperpolarization-activated cyclic nucleotide-gated potassium channel (HCN) in the transcriptome of the green crab *Carcinus maenas* and subsequent performance of quantitative real-time PCR revealed the ubiquitous expression of this channel in this species. Even though mRNA expression levels in the cerebral ganglion were found to be approximately 10 times higher compared with all other tissues, posterior gills still expressed significant levels of HCN, indicating an important role for this transporter in branchial ion regulation. The relatively unspecific K^+-channel inhibitor Ba^{2+}, as well as the HCN-specific blocker ZD7288, as applied in gill perfusion experiments and electrophysiological studies employing the split gill lamellae revealed the presence of at least two different K^+/NH_4^+-transporting structures in the branchial epithelium of *C. maenas*. Furthermore, HCN mRNA levels in posterior gill 7 decreased significantly in response to the respiratory or metabolic acidosis that was induced by acclimation of green crabs to high environmental P_{CO_2} and ammonia, respectively. Consequently, the present study provides first evidence that HCN-promoted NH_4^+ epithelial transport is involved in both branchial acid-base and ammonia regulation in an invertebrate.

KEY WORDS: Ammonia, Gill perfusion, HCN, Hypercapnia, HEA

INTRODUCTION

Potassium channels form a diverse family of ubiquitously expressed transmembrane proteins that are crucial for a number of important physiological functions (Tian et al., 2014). In particular, K^+ fluxes are essential for the membrane excitability of neurons and muscles (Choe, 2002). In the crustacean gill epithelium, K^+ channels have been identified to participate in the establishment of an electrochemical gradient over the basolateral membrane mainly generated by a basolateral Na^+/K^+-ATPase (Onken et al., 1991; Riestenpatt et al., 1996). Furthermore, apical K^+ channels seem to co-localize with apical $Na^+/K^+/2Cl^-$ (NKCC) to allow K^+ circulation and thereby an uptake of Na^+ and Cl^- in crustaceans (Riestenpatt et al., 1996; Onken et al., 2003). Because of the presence of apical NKCC and apical K^+ channels, as well as the accompanying basolateral Cl^- channel, the moderately leaky gill epithelium of *C. maenas* has been compared with the thick ascending limb (TAL) of the mammalian kidney (Riestenpatt et al., 1996). The apical K^+ channel present in the TAL is a member of the inwardly rectifying K^+ channel family K_{IR} (Kir1.1) and promotes apical efflux of K^+ to energize the apical NKCC. Additionally, Kir4.1/5.1 has been identified to be co-localized basolaterally with the Na^+/K^+-ATPase in the kidney's distal tubule, providing a basolateral back flow of K^+ out of the cell into the body fluids to maintain the electrochemical gradient (Hibino et al., 2010).

As a general, relatively unspecific inhibitor of K^+ currents, apical 15 mmol l^{-1} Ba^{2+} reduced the short-circuit current (I_{SC}) and trans-epithelial conductance (G_{TE}) of split gill lamellae of *C. maenas* (Riestenpatt, 1995; Riestenpatt et al., 1996). In gills of *Neohelice* (*Chasmagnathus*) *granulata*, basolateral application of 10 mmol l^{-1} $BaCl_2$ altered I_{SC} without affecting the conductance, but had no effect when applied apically even though apical Cs^+, another unspecific K^+ channel blocker, resulted in a significant decrease of I_{SC} (Onken et al., 2003). At these relatively high concentrations, Ba^{2+} is believed to target voltage-gated/delayed-rectifier K^+ channels (Rudy, 1988; Wollmuth, 1994), while specifically inhibiting Ca^{2+}-activated K^+ channels and K^+ channels of the K_{IR} family only in lower concentrations of up to 100 µmol l^{-1} (Wollmuth, 1994; Franchini et al., 2004). The fact that the K^+-dependent current in the *C. maenas* gill could be more potently inhibited by 10 mmol l^{-1} apical Cs^+, however, indicates the presence of at least two, a Ba^{2+}-sensitive and a Ba^{2+}-insensitive K^+ channel population (Riestenpatt, 1995; Riestenpatt et al., 1996). Furthermore, application of Ba^{2+} in split gills of the Chinese mitten crab, *Eriocheir sinensis*, resulted in a complex di-phasic response of the short-circuit current I_{SC} (Onken et al., 1991), also indicating the participation of more than one kind of K^+ channel.

In addition to their role in osmoregulation, basolateral K^+ channels also participate in branchial ammonia excretion in *C. maenas*, with NH_4^+ substituting for K^+ because of its similar size and charge (Lignon, 1987; Skou, 1960; Weihrauch et al., 1998). Apical application of Cs^+, however, did not affect branchial ammonia excretion in this species (Weihrauch et al., 1998). Furthermore, branchial ammonia regulation in *C. maenas* has been observed to be closely linked to acid-base regulation (Fehsenfeld and Weihrauch, 2013), but the specific role of K^+ channels in this context is not clear.

Interestingly, a K^+ channel of the hyperpolarization-activated cyclic nucleotide-gated channel family (HCN2) has recently been shown to be involved in acid-base and ammonia regulation in the collecting duct of the mammalian kidney (Carrisoza-Gaytán et al.,

[1]Department of Zoology, University of British Columbia, 6720 University Blvd, Vancouver, British Columbia, Canada V6T 1Z4. [2]Department of Biological Sciences, University of Manitoba, 190 Dysart Road, Winnipeg, Manitoba, Canada R3T 2N2.

*Author for correspondence (Fehsenfeld@zoology.ubc.ca)

Received 6 November 2015; Accepted 11 January 2016

Journal of Experimental Biology (2016) 219, 887-896 doi:10.1242/jeb.134502

2011). Although to date, HCN2 has been mainly associated with pacemaker activities (DiFrancesco, 1993), Carrisoza-Gaytán and colleagues (2011) showed that this gene is also expressed in the basolateral epithelium of rat kidney cells and is capable of promoting NH_4^+ transport over the membrane, thus participating in mammalian renal pH homeostasis.

The present study aims to investigate the role of K^+ channels in branchial acid-base regulation of the osmoregulating green crab *C. maenas*, and particularly of an HCN-like protein as identified in the transcriptome. By application of two different K^+ channel inhibitors, Ba^{2+} and the HCN-specific ZD7288, acid-base and ammonia regulatory properties of the gill epithelium will be characterized with respect to K^+ and NH_4^+ transport. A potential role for K^+ channels, and specifically for HCN, will be evaluated.

MATERIALS AND METHODS

Identification and gene tree analysis of CmHCN

To identify potential candidates for the hyperpolarization-activated cyclic nucleotide-gated potassium channel family in *C. maenas* (CmHCN), the partial amino acid sequence for the hyperpolarization-activated ion channel of *Cancer borealis* (GenBank accession no. AAZ80094.3) was used as assembly scaffold for a recently generated transcriptome for *C. maenas* (Verbruggen et al., 2015) using the basic local alignment search tool (BLAST) feature in Geneious© version 7.1 (Biomatters Limited, Auckland, New Zealand). Accordingly, potential candidates for the basic voltage-gated (K_V), inward-rectifying (K_{IR}), two-pore domain (K_{2P}) and Ca^{2+}-activated (K_{Ca}) K^+ channels were identified in the *C. maenas* transcriptome using the sequences for the potassium voltage-gated channel subfamily H member 6 isoform 1 (accession no. NP_110406.1) and the ATP-dependent inward-rectifying potassium channel KIR4.1 and 5.1 of *Homo sapiens* (accession nos AAB07046.1 and AAF73240.1), the acid-sensitive two-pore domain K^+ channel dTASK-7 of *Drosophila melanogaster* (accession no. CAI72673.1), as well as the calcium-activated potassium channel of *C. borealis* (accession no. AAZ80093.4).

The best protein model for the gene analysis on all HCN candidates as listed in Table 1 was chosen according to the test function provided in MEGA 6.06 (Tamura et al., 2013). Subsequently, a gene tree was constructed in MEGA 6.06, applying the maximum likelihood method using the gamma-distributed GL model with invariant sites (LG+I+G; Le and Gascuel, 2008). A matrix of pairwise distances estimated using a JTT model (Jones et al., 1992) was used to automatically generate an initial tree(s) for the heuristic search by applying neighbour-joining and BioNJ algorithms and subsequently selecting the topology with the superior log-likelihood value. Evolutionary rate differences among sites were modelled by discrete gamma distribution (six categories). All positions with less than 95% site coverage were eliminated (i.e. less than 5% alignment gaps, missing data and ambiguous bases were allowed at any position). Bootstrap analyses were performed with 1000 replicates.

Animals

For gill perfusion experiments, male green crabs, *Carcinus maenas* (Linnaeus 1758), were caught in traps in the Kiel Fjord (Baltic Sea) in front of the GEOMAR pier (west shore building, 54°19.8′N, 10°9.0′E) at 3–4 m depth in May 2012 (collection permit issued September 2009, file no. V313-72241.121-19). Animals were kept in ca. 250 litre flow-through tanks in a climate chamber at GEOMAR, directly fed by water from the Kiel Fjord (salinity=14.3±0.0 ppt, temperature=17.2±0.4°C, pH_{NBS}=7.96±0.03, P_{CO_2}=96±7 Pa), until gill perfusions were performed (see below). Green crabs were fed *ad libitum* with blue mussels, *Mytilus edulis*, twice per week. Animals were starved for a minimum of 2 days before experiments.

For quantitative real-time PCR and Ussing chamber experiments, male green crabs were caught in Barkley Sound at the opening of the Pipestem Inlet (Vancouver Island, BC, Canada) in summer 2013 under Department of Fisheries and Oceans collection permit XR-235-2013, and transported back to Winnipeg, MB, Canada. They were kept at the animal holding facility of the University of Manitoba in aerated 1200 litre tanks with artificial seawater adjusted to a salinity of 32 ppt at 14°C (Seachem Marine Salt®) until experimentation. For acclimation to dilute salinity of 11 ppt, eight animals were transferred into a 120 litre tank for a minimum of 7 days and fed *ad libitum* with squid once a week. Water was exchanged at least every second day and always on the day after feeding. Green crabs were starved for a minimum of 2 days prior to experiments.

For subsequent acclimation of green crabs to high environmental ammonia (HEA) for 7 days, the brackish water of the 120 litre tanks was enriched with 1 mmol l^{-1} NH_4Cl. Water was exchanged on a daily basis and animals were not fed during HEA acclimation.

Quantitative real-time PCR

Gene expression analysis was performed on tissues obtained from animals held at University of Manitoba. Posterior gill 7 and all other tissue samples of osmoregulating *C. maenas* (11 ppt) acclimated to control conditions and HEA (1 mmol l^{-1} NH_4Cl, 7 days) were harvested from animals acclimated as described above, while samples for hypercapnia-acclimated green crabs (400 Pa) were used as described in the recent study by Fehsenfeld and Weihrauch (2013). Tissue samples representing anterior and posterior gills were generated by pooling equal tissue amounts of the respective gills prior to isolating the RNA (gills 4 and 5 for anterior gills, and gills 7, 8 and 9 for posterior gills).

Briefly, total RNA was isolated under RNase-free conditions using TRIZOL (Invitrogen, Carlsbad, CA, USA). Following DNase I (Ambion™, Thermo Fisher Scientific, Pittsburgh, PA, USA) treatment, regular PCR was performed to ensure the absence of DNA traces (RbS-3 primers; forward: 5′ GTCCCTTTTCACCAA-GGACA; reverse: 3′ CAAGGCCAAACTCAACA GGTT). Subsequently, verified DNA-free RNA was transcribed with the iScript cDNA synthesis kit (Bio-Rad, Mississauga, ON, Canada). Quantitative real-time PCR (qPCR) was performed on 20 ng cDNA and a final primer concentration of 0.4 µmol l^{-1} in 15 µl reactions with the SSO FastEvaGreen Supermix (Bio-Rad). The gene-specific primers for CmHCN were designed based on the identified transcriptome contig (forward: 5′ GTCTTCATGCGCA-TCTTCAA; reverse: 5′-GTTGATTGCCACCCAAGAGT) and resulted in the expected specific 123 bp fragment. The primers were ensured to result in a single signal in the qPCR by adding a melting curve analysis following the regular qPCR. In every qPCR run, a negative control (no template) was included to verify that the assay was not contaminated, as well as one of the standards treated as an unknown sample to ensure homogeneous performance. A standard curve was included in each qPCR run based on a dilution series of known quantities of the respective gel-extracted gene fragment (0.01–100 fg; QIAquick Gel Extraction Kit, Qiagen). Additionally, the housekeeping gene ribosomal RbS-3 was used for internal normalization of hypercapnia-related tissues in accordance with Fehsenfeld and Weihrauch (2013). No housekeeping gene (i.e. RbS-3, arginine kinase) with constant mRNA expression levels

Journal of Experimental Biology

Journal of Experimental Biology (2016) 219, 887-896 doi:10.1242/jeb.134502

Table 1. Information on the potassium channels as included in the gene tree analysis as depicted in Fig. 2

Species	(Infra) Class	Accession no.	Description
Homo sapiens	Mammalia	NP_001185.3	HCN (2)
		NP_110406.1	K_V (H6 isoform 1)
		Q9H427.2	K_{2P} (KT3.3)
		NP_002238.2	K_{Ca} (subunit alpha-1b)
		AAB07046.1	K_{IR} 4.1
		AAF73240.1	K_{IR} 5.1
Mus musculus	Mammalia	NP_032252.1	HCN (2)
		NP_001032801.1	K_V (H6)
		AAC53367.1	K_{2P} (TWIK-related)
		NP_001240307.1	K_{Ca} (subunit alpha-1.22)
		BAA92432.1	K_{IR} 4.1
		BAA34723.1	K_{IR} 5.1
Danio rerio	Teleostei	XP_686078.4	HCN
		NP_998002.1	K_V (H6)
		NP_001122021.1	K_{2P} (K9)
		NP_001139072.1	K_{Ca} (subunit alpha-1)
		NP_001092204.1	K_{IR} 4.1
		NP_001265731.1	K_{IR} (J2a)
Strongylocentrotus purpuratus	Echinoidea	NP_001028182.1	HCN
		XP_011669414.1	K_V (H7 isoform X1)
		XP_782284.2	K_{2P} (sup-9-like)
		XP_011666091.1	K_{Ca} (subunit alpha-1)
		XP_789112.1	K_{IR} (12)
Aedes aegypti	Insecta	XP_001658860.1	HCN (AAEL008056-PA)
		XP_001653553.1	K_V (AAEL001542-PA)
		XP_001652733.1	K_{2P} (AAEL007386-PA)
		AAL40812.1	K_{Ca} (AAEL003765-PA)
		AGA61793.1	K_{IR} (1)
Drosophila melanogaster	Insecta	AAX78393.1	HCN (DMIH-A1B1C1)
		NP_476713.1	K_V (seizure, isoform A)
		CAI72673.1	K_{2P} (dTASK-7)
		AAA28651.1	K_{Ca}
		CAC87638.1	K_{IR}
Daphnia pulex	Branchiopoda	EFX81385.1	HCN (DAPPUDRAFT_2754)
		EFX90436.1	K_V (DAPPUDRAFT_39704)
		EFX84367.1	K_{2P} (DAPPUDRAFT_25421)
		EFX85873.1	K_{Ca} (DAPPUDRAFT_313756)
		EFX88146.1	K_{IR} (DAPPUDRAFT_311738)
Carcinus maenas	Malacostraca	GBXE01087917.1	HCN (Transcriptome contig)
		GBXE01103936.1	K_V (Transcriptome contig)
		GBXE01029129.1	K_{2P} (Transcriptome contig)
		GBXE01102019.1	K_{Ca} (Transcriptome contig)
		GBXE01116654.1	K_{IR} (Transcriptome contig)
Cancer borealis	Malacostraca	AAZ80094.3	HCN (HAIC)
		AAZ80093.4	K_{Ca}

Accession numbers are according to GenBank and specific descriptions are based on the NCBI protein database. HCN, potassium/sodium hyperpolarization-activated cyclic nucleotide-gated channel; K_V, voltage-gated potassium channel; K_{2P}, two-pore domain K^+-channel; K_{Ca}, calcium-activated potassium channel; K_{IR}, inwardly rectifying potassium channel.

could be identified for HEA-acclimated green crabs. Hence, absolute quantification was solely assessed using the included standard curve. In this case, a standard curve based on diluted cDNA samples was performed to ensure comparable amplification efficiency [PCR fragments: 99.4±0.2% (N=3); cDNA templates: 100.5±0.7% (N=3)].

Perfusion experiments on isolated posterior gill 7

For gill perfusion experiments in Kiel, hemolymph ammonia, hemolymph carbonate system parameters, as well as hemolymph cation concentrations (Na^+, K^+ and Ca^{2+}; flame photometer analysis performed by T. Stegmann, Institute of Physiology, Christian-Albrechts-University Kiel) of control green crabs were assessed for the adjustment of the perfusion solution as described in Fehsenfeld and Weihrauch (2013) to account for *in vivo* conditions of the Baltic Sea individuals. Accordingly, the perfusion solution consisted of (in mmol l^{-1}): 340 NaCl, 9 $CaCl_2$, 7 $MgCl_2$, 9 KCl, 14 $NaHCO_3$, 0.13 NH_4Cl, 0.5 glutamine, 0.5 glucose and 0.1 glutathione. The pH (NBS scale) was adjusted to 7.9. Posterior gills (no. 7) were perfused according to the procedure described in Fehsenfeld and Weihrauch (2013), following the technique of Siebers et al. (1985). Each perfusion consisted of a control step, followed by the application of the respective inhibitor and a third wash-out step to ensure the survival of the gill tissue. Each perfusion step allowed for 10 min adjustment of the gill, after which the perfusate was collected for 30 min. To block basolateral K^+ channels, $BaCl_2$ was applied basolaterally in the second perfusion step at a concentration of 12 mmol l^{-1} (Schirmanns and Zeiske, 1994; Riestenpatt, 1995; Riestenpatt et al., 1996; Onken et al., 2003). The inhibitor ZD7288 (4-ethylphenylamino-1,2-dimethyl-6-methylaminopyrimidinium

Journal of Experimental Biology (2016) 219, 887-896 doi:10.1242/jeb.134502

chloride) was applied basolaterally at a concentration of 10 µmol l^{-1} to specifically block the K^+ current generated by the identified HCN, according to Carrisoza-Gaytán et al. (2011). Gill ammonia excretion rates were calculated based on the difference in the perfusate compared with the perfusion solution. Perfusate proton concentration was calculated based on the pH, whereas perfusate P_{CO_2} and HCO_3^- were calculated using the equations and constants following Truchot (1976). An increase in perfusate [H^+], CO_2 and/or [HCO_3^-] in comparison to the initial perfusion solution was considered equivalent to a decrease in excretion.

Ussing chamber experiments on split gill lamellae (posterior gill 7)

Ussing chamber experiments were performed at room temperature in Winnipeg, Canada. Single gill lamellae of posterior gill 7 were split according to Schwarz and Graszynski (1989) and mounted in the EM-CSYS-6 Ussing chamber system (Physiologic Instruments, San Diego, CA, USA) with specific sliders (P2308), providing a circular aperture of 1 mm that resulted in an open epithelial surface area of 8×10^{-3} cm^2. Silicon grease was used to seal the edges of the preparation to prevent potential edge damage. Preparations were aerated throughout the experiment. Providing six channels and chambers, the EM-CSYS-6 Ussing chamber system together with the automatic clamping device (VCC 600, Physiologic Instruments) allowed for six split gill lamellae to be investigated in parallel in one experimental run.

Symmetrical conditions were used to account for only active ion transport, with the following identical crab saline being applied to both the apical and basolateral sides (in mmol l^{-1}): 248 NaCl, 5 $CaCl_2$, 4 $MgCl_2$, 5 KCl, 2 $NaHCO_3$, 5 HEPES and 2 glucose (after Riestenpatt et al., 1996). The pH_{NBS} was adjusted to 7.9. Two pairs of Ag/AgCl electrodes were connected to the preparation via agar bridges (3% agarose in crab saline to avoid diffusive effects of KCl): one pair served to determine the trans-epithelial potential difference (PD_{TE}), and the second pair served as current electrodes to short-circuit the PD_{TE} with the VCC600. The reference electrode was positioned at the basolateral side. Before the tissue was introduced into the experimental setup, the voltage offset between paired electrodes was set to 0.0. It was ensured that the agar bridges did not produce excessive resistance by passing current in this open setup (resulting in ca. 60 µA). Using the fluid resistance compensation function of the clamping device, the potentiometer was adjusted so that the voltage was again nullified while passing current. The resistance of the crab saline (R_S) could be read from the potentiometer knob and was determined as 8.2 ±0.1 Ω cm^{-2}. After mounting the six split gill lamellae, the (area-) corrected short-circuit current I_{SC} (as a measure of ion/charge movements over the gill epithelium; Riestenpatt et al., 1996) was directly recorded simultaneously for every channel using Acquire Analyze software (version 2.2). Voltage pulses (5 mV every 60 s for 1 s) were applied to assess the epithelial conductance {$G_{TE}=1/R_{TE}$, $R_{TE}=[(\Delta V/\Delta I)-R_S]=[(5\text{ mV}/\Delta I_{SC})-8.2\ \Omega\ cm^{-2}]$, where R_{TE} is the transepithelial resistance and ΔV is the amplitude of the voltage pulse}.

The dose–response curve for ZD7288 was obtained by increasing the concentration basolaterally in a step-wise fashion. As soon as I_{SC} levelled off for one concentration (ca. 10–15 min) and remained stable for >1 min, the next higher concentration was applied. In case of the dose–response curve for $BaCl_2$, preceding the basolateral application of each concentration of $BaCl_2$ was the application of an equivalent concentration of choline chloride apically to account for potential Cl^--dependent changes in I_{SC}. To account for time effects on the I_{SC}, one split gill lamella per experimental run was kept under control conditions during the full duration of the experiment.

Fig. 1. ClustalW alignment of *Carcinus maenas* HCN and *Homo sapiens* HCN2 proteins. Indicated in the sequence are the voltage-dependent potassium channel motif PLNO3192 (underlined), the Crp motif for the predicted cNMP/cAMP binding site (grey background), and the binding sites Ala425 and Leu432 for the inhibitor ZD7288 (black boxes) after Cheng et al. (2007). '*', single, fully conserved residue; ':', conservation of strong groups; '.', conservation of weak groups as designated by Biology WorkBench (version 3.2, http://seqtool.sdsc.edu/CGI/BW.cgi).

Statistics

All statistical analyses were performed with PAST3 (Hammer et al., 2001). Data sets were tested for normal distribution (Shapiro–Wilk test) and homogeneity of variances (*F*-test) to qualify for parametrical testing. If one or both requirements were not met, data were log transformed. If log transformation still did not result in a data set appropriate for parametric testing, non-parametrical tests were applied instead. For comparison of single means, a paired *t*-test was applied (gill perfusion, mRNA expression changes stressors), whereas Kruskal–Wallis with pairwise Mann–Whitney comparisons was used to compare multiple means (tissue expression). Dose–response curves were evaluated by repeated measures ANOVA with *post hoc* Tukey's pairwise comparisons after verifying a normal distribution (Shapiro–Wilk test) and homogeneity of variances (Levene's test). All results were considered significant at $P<0.05$. Graphs were generated using the software Inkscape, version 0.48 (https://inkscape.org/). The dose–response curve for Ba^{2+} was generated by GraphPad Prism version 6.00 for Windows (GraphPad Software, San Diego, CA, USA, www.graphpad.com).

RESULTS

Identification of CmHCN and gene tree analysis

The two different identified contigs (resulting in an open reading frame of >100 amino acids) in the green crab transcriptome resembling HCN, GBXE01087917.1 (326 amino acids) and GBXE01153810.1 (148 amino acids), aligned to different regions of the HCN sequence of *C. borealis* (positions 291–712 versus 66–213, respectively) and HCN2 of *H. sapiens* (positions 360–659 versus 180–299, respectively). Only GBXE01087917.1 contained the specific motifs for voltage-gated potassium channels (PLN03192) and the cyclic nucleotide-monophosphate binding domain (cAMP/cNMP/Crp) as determined by the NCBI protein BLAST tool and was therefore chosen for further analysis. The partial 326 amino acid sequence for CmHCN was highly conserved and resembled the human HCN2 with 69% identity and 83% overall conserved domains (Fig. 1). The major binding sites for ZD7288

Journal of Experimental Biology (2016) 219, 887-896 doi:10.1242/jeb.134502

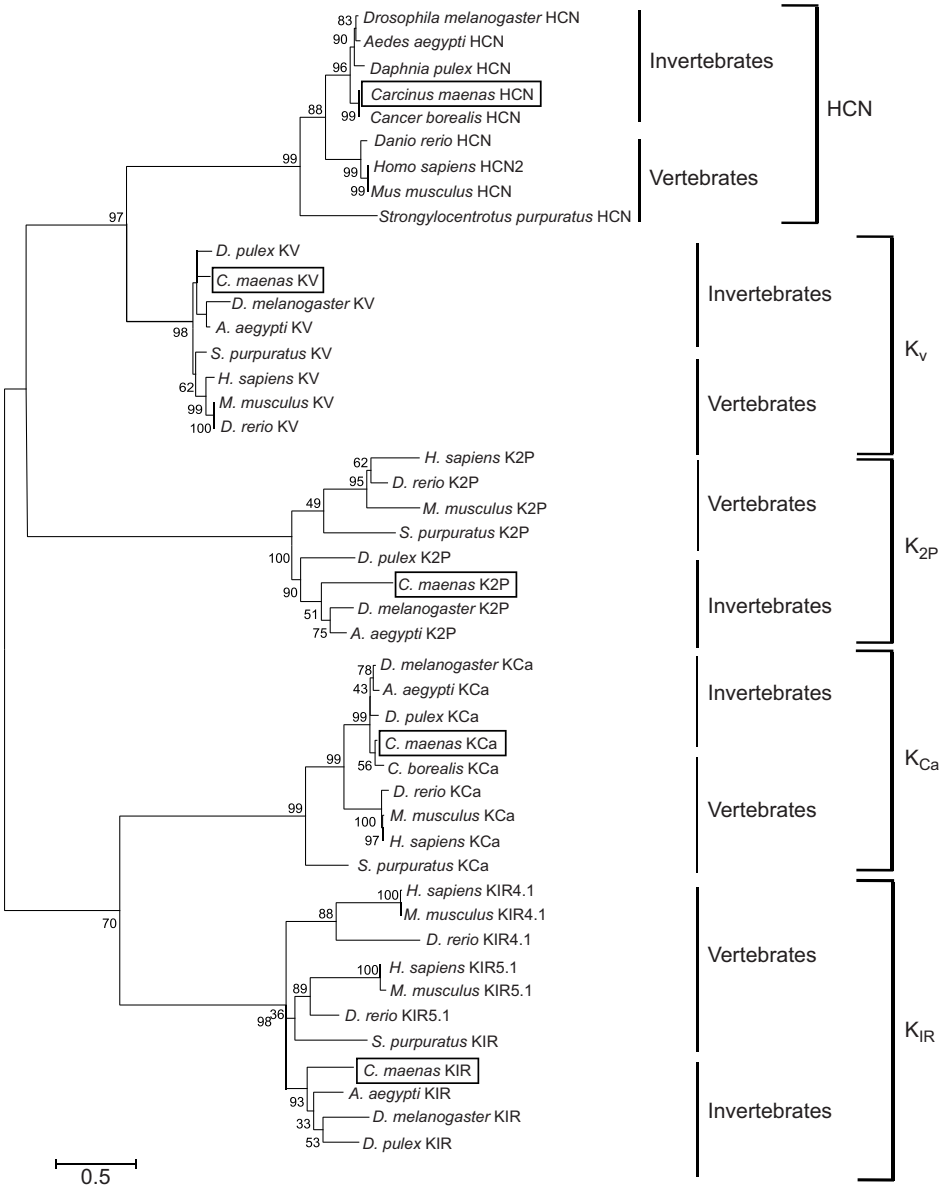

Fig. 2. Molecular gene tree analysis of potassium channels in vertebrates and invertebrates. The maximum likelihood analysis was conducted using the LG model (Le and Gascuel, 2008) based on pairwise distances calculated by the JTT model (Jones et al., 1992) as implemented in MEGA6.06 (Tamura et al., 2013). The tree with the highest log-likelihood of –6915.8448 is shown and drawn to scale, so that the branch lengths represent the number of substitutions per site (scale bar). Numbers beside the branches indicate the percentage of trees that clustered together in the displayed way. HCN, hyperpolarization-activated cyclic nucleotide-gated potassium channel; K_V, voltage-gated potassium channel; K_{2P}, two-pore domain potassium channel; K_{Ca}, calcium-activated potassium channel; K_{IR}, inward-rectifying potassium channel.

were identified as Ala-425 and Leu-432, as recently described by Cheng et al. (2007).

For each of the four classes of K^+ channels (K_V, K_{IR}, K_{2P} and K_{Ca}), a respective contig could be identified in the transcriptome of *C. maenas* as generated by Verbruggen et al. (2015). A discrete gamma distribution was used to model evolutionary rate differences among sites between all sequences included in the gene tree analysis (six categories; $+G$, parameter=3.3). The rate variation model allowed for some sites to be evolutionarily invariable ([$+I$], 1.1% sites). All positions with less than 95% site coverage were eliminated, resulting in a total of 141 positions in the final dataset. For all included invertebrate and vertebrate sequences, the respective K^+-channel families formed distinct monophyletic groups (Fig. 2). As expected, the HCNs represented a distinct (sub)family of the voltage-gated K^+ channels. Furthermore, the gene tree analysis revealed that *C. maenas* grouped with the other arthropod channels in all cases. Although four different HCNs could be found in mammals (only HCN2 included, other data not shown), arthropods seem to express only one HCN. A similar observation was made for the K_{IR}-related proteins of the arthropods, which seemed to resemble KIR5.1 channels as found in mammals and fish.

CmHCN was observed to be ubiquitously expressed in all analyzed tissues. Although the cerebral ganglion exhibited the highest mRNA expression levels (ca. 10-fold compared with the other tissues), posterior gills still exhibited significant levels of the transcript (Fig. 3).

Effects of K^+-channel inhibitors on branchial acid-base regulation, ammonia excretion and the short-circuit current

The excretion of ammonia, CO_2 and HCO_3^- as well as the concentration of H^+ in the perfusate were significantly affected by both Ba^{2+} and the HCN-specific ZD7288 in posterior gill 7 of osmoregulating green crabs when applied basolaterally (Fig. 4). The degree of inhibition, however, varied with both inhibitors. Whereas branchial ammonia excretion decreased to a greater extent with the application of Ba^{2+} (ca. 70% versus 40% with ZD7288; Fig. 4A), excretion of acid equivalents (as equivalent to accumulation of protons in the hemolymph) decreased more drastically under the

Journal of Experimental Biology (2016) 219, 887-896 doi:10.1242/jeb.134502

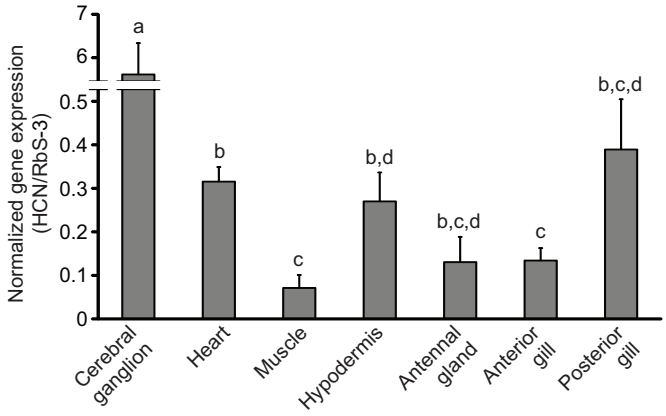

Fig. 3. Normalized tissue expression of CmHCN in *Carcinus maenas* acclimated to brackish water (11 ppt). mRNA expression was normalized to the ribosomal gene RbS-3. Values are given as means±s.e.m. Significant differences are indicated by different lowercase letters (Kruskal–Wallis test with pairwise Mann–Whitney, P<0.05, N=4–5).

influence of ZD7288 (1.3-fold; Fig. 4B). The effect of Ba^{2+} on perfusate proton concentration was small, yet significant. In regard to CO_2 excretion, the application of both inhibitors resulted in a significant, ca. 1.1-fold increase of P_{CO_2} in the perfusate (equivalent to a 1.1-fold decrease in excretion; Fig. 4C). The most pronounced difference between Ba^{2+} and ZD7288 was observed in relation to HCO_3^-: whereas ZD7288 resulted in a small, but significant increase of 5% in the perfusate, Ba^{2+} resulted in the opposite response, namely, a 5% increase in perfusate [HCO_3^-] (reduced excretion; Fig. 4D).

Split gill lamellae of osmoregulating green crabs employed in the present study generated an outside positive PD_{TE} of 4.5±0.4 mV (n=17) and an inward negative I_{SC} of −445±28 µA cm^{-2} (n=17) in the Ussing chamber setup, indicating a net flux of negative charge from the apical to the basolateral side. The corresponding

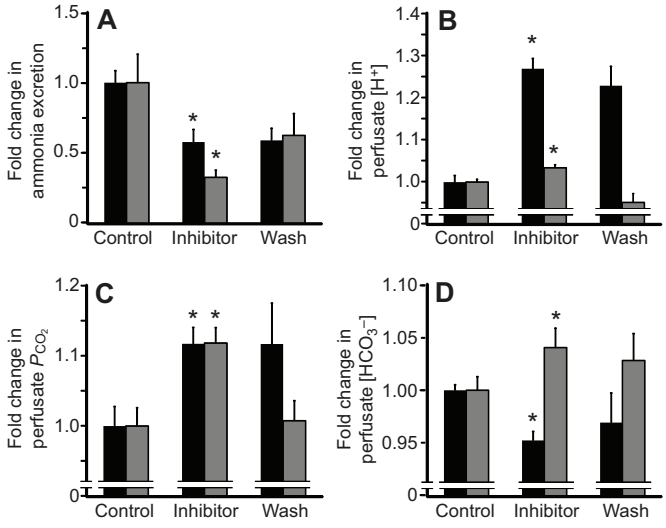

Fig. 4. Changes in ammonia and acid-base excretory patterns by isolated perfused posterior gill 7 of brackish-water (15 ppt) acclimated *Carcinus maenas* applying inhibitors for potassium channels. (A) Ammonia excretion rates, (B) perfusate [H^+], (C) perfusate P_{CO_2} and (D) perfusate [HCO_3^-] during control perfusion, during application of basolateral inhibitors, and during the wash step. The HCN-specific inhibitor ZD7288 (black bars) was applied at 10 µmol l^{-1}, whereas the more universal inhibitor $BaCl_2$ (grey bars) was applied at a concentration of 12 mmol l^{-1}. Values are given as means± s.e.m. Asterisks denote a significant difference between the control and the inhibitor step of the respective inhibitor (paired t-test with P<0.05, N=6).

conductance G_{TE} accounted for 35.0±2.5 mS cm^{-2} (n=17). Although G_{TE} exhibited similar values in all preparations, I_{SC} was more variable, with values between −196 and −634 µA cm^{-2}. Without influence of any inhibitor and only accounting for changes over time, the I_{SC} remained relatively stable over the experimental time period and decreased on average by 1.7±0.4% per 10 min (n=5). The maximal overall decrease was observed in one of the runs during the initial 20 min and accounted for 5% of the initial I_{SC}.

When applied basolaterally on split gill lamellae (gill 7) in Ussing chamber experiments, both inhibitors (Ba^{2+} and ZD7288) reduced the initial short-circuit current in a dose-dependent manner, as can be seen in the exemplary time curves (Figs 5, 6) as well as the dose–response curves (Fig. 7). The conductance remained relatively stable and only seemed to decrease slightly with higher concentrations of $BaCl_2$.

For the dose–response curves, all measurements for I_{SC} have been corrected for the observed maximum time effect of −5% per 20 min. In the case of Ba^{2+}, the basolateral inhibition of I_{SC} followed typical Michaelis–Menten kinetics and could be fitted by the Hill equation with ΔI_{SCmax}=−346.9 µA cm^{-2} (73% inhibition) and IC_{50}=0.76 mmol l^{-1}. The application of ZD7288 resulted in an almost linear decrease of the I_{SC} and hence was not fitted by a typical dose–response curve. The maximum inhibition of I_{SC} at 10 µmol l^{-1} (plateauing after 1 µmol l^{-1}) accounted for 30% of the initial I_{SC} (ΔI_{SCmax}=−120.2 µA cm^{-2}) and the basolateral application of ZD7288 resulted in an IC_{50} of 6×10^{-7} mmol l^{-1}.

CmHCN in response to environmental stressors

mRNA levels of CmHCN in posterior gill 7 were significantly downregulated in green crabs exposed to 7 days of either high environmental P_{CO_2} (hypercapnia, 400 Pa; ca. 50% reduction) or elevated environmental ammonia (1 mmol l^{-1} NH_4Cl HEA, ca. 80% reduction; Fig. 8).

DISCUSSION

Potential K^+-permeable structures in the gill epithelium of *Carcinus maenas*

In studies to date, the presence of K^+ channels in the gill epithelium of decapod crustaceans has only been verified by ion flux and short-circuit current studies on split gill lamellae applying the inhibitors Ba^{2+} and Cs^+ (Onken et al., 1991, 2003; Riestenpatt et al., 1996; Weihrauch et al., 1998, 1999). Because of its similar radius in comparison to K^+, Ba^{2+} is able to enter the channel pore and bind to the selection filter motif (SF4) domain of the respective K^+ channels, thereby competing with K^+ and blocking its binding site more potently because of its dual positive charge (Rossi et al., 2013). As Fig. 2 shows, representatives for K_{Ca}, K_{2P}, K_{IR}, K_V and HCN can be found throughout the animal kingdom, and, based on transcriptome analysis, also in the green crab *C. maenas*. However, to our knowledge, the specific nature of K^+-promoting membrane channels in the crustacean gill has not been investigated to date.

The identified CmHCN, as described in the present study, thus provides the first (partial) sequence-based characterization of a potential K^+/NH_4^+ channel in a decapod crustacean and documents its involvement in branchial acid-base and ammonia regulation.

Importantly, Fig. 1 shows clearly that CmHCN exhibits the respective binding sites for ZD7288, Ala-425 and Leu-432, as described by Cheng et al. (2007). Even though the latter differs from the mammalian Ile-432, the authors of that study showed that substitution of Ile with Leu did not shift the IC_{50} significantly. Accordingly, this provided the basis for the functional studies applying ZD7288 in gill perfusion and Ussing chamber experiments.

Journal of Experimental Biology

Journal of Experimental Biology (2016) 219, 887-896 doi:10.1242/jeb.134502

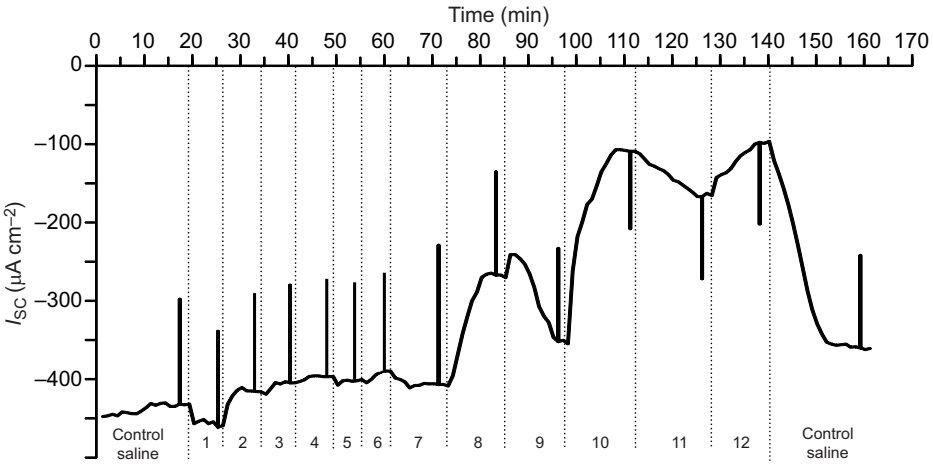

Fig. 5. Representative time course for the changes of short-circuit current (I_{SC}) across split lamellae of posterior gill 7 of *Carcinus maenas* applying apical choline chloride and basolateral $BaCl_2$. I_{SC} is corrected for fluid resistance, but not for the general decrease over time (see Materials and methods for details). The vertical current deflections reflect the conductance as assessed by the application of 5 mV voltage pulses. (1) 10 µmol l^{-1} apical choline chloride; (2) 10 µmol l^{-1} apical choline chloride and 10 µmol l^{-1} basolateral $BaCl_2$; (3) 100 µmol l^{-1} apical choline chloride and 10 µmol l^{-1} basolateral $BaCl_2$; (4) 100 µmol l^{-1} apical choline chloride and 100 µmol l^{-1} basolateral $BaCl_2$; (5) 1 mmol l^{-1} apical choline chloride and 100 µmol l^{-1} basolateral $BaCl_2$; (6) 1 mmol l^{-1} apical choline chloride and 1 mmol l^{-1} basolateral $BaCl_2$; (7) 5 mmol l^{-1} apical choline chloride and 1 mmol l^{-1} basolateral $BaCl_2$; (8) 5 mmol l^{-1} apical choline chloride and 5 mmol l^{-1} basolateral $BaCl_2$; (9) 10 mmol l^{-1} apical choline chloride and 5 mmol l^{-1} basolateral $BaCl_2$; (10) 10 mmol l^{-1} apical choline chloride and 10 mmol l^{-1} basolateral $BaCl_2$; (11) 20 mmol l^{-1} apical choline chloride and 10 mmol l^{-1} basolateral $BaCl_2$; (12) 20 mmol l^{-1} apical choline chloride and 20 mmol l^{-1} basolateral $BaCl_2$.

Molecular characterization of CmHCN

As seen by the sequence and gene tree analysis, the level of conservation of the HCN sequence between arthropods and vertebrates in general, and *C. maenas* and *H. sapiens* specifically, is significant. A similar level of conservation between invertebrate and vertebrate proteins is found in other important membrane transporters such as the α-subunit of the Na^+/K^+-ATPase, one of the most important epithelial proteins (*C. maenas* versus *Homo sapiens*, 79% identity and 89% overall conserved domains, NCBI). Consequently, HCN can be hypothesized to inherit a significant role in the course of evolution regarding epithelial ion transport.

In collecting ducts of rat renal cortex and medulla – structures that are responsible for both ammonia and acid-base regulation in mammals (Weiner and Verlander, 2013) – HCN2 has recently been observed to transport not only K^+, but also NH_4^+ (Carrisoza-Gaytán et al., 2011). As the major ion, ammonia and acid-base regulatory organ (Larsen et al., 2014), the crustacean gill resembles many of the transport processes that are observed in the mammalian kidney (Riestenpatt et al., 1996) and it is therefore not surprising that, in addition to in the cerebral ganglion, significant mRNA expression levels of HCN can be found in the osmoregulatory posterior gills of *C. maenas*. Interestingly, the difference of CmHCN mRNA levels between anterior and posterior gills (ca. fivefold) mirrors what is seen for Na^+/K^+-ATPase (NKA) activity in these tissues (ca. 2 versus 11 µmol P_i mg protein^{-1} h^{-1}), emphasizing the postulated close relationship between basolateral NKA and K^+ channels in mammalian (Hibino et al., 2010) as well as invertebrate epithelia (Riestenpatt et al., 1996).

Furthermore, the detected downregulation of the mammalian renal HCN2 mRNA in response to chronic metabolic acidosis in rats (Carrisoza-Gaytán et al., 2011) was also observed in the present study in the gills of *C. maenas* in response to the metabolic acidosis resulting from acclimation to high environmental ammonia (unpublished data). In addition, a role for CmHCN in general acid-base regulation is indicated by its significant downregulation as

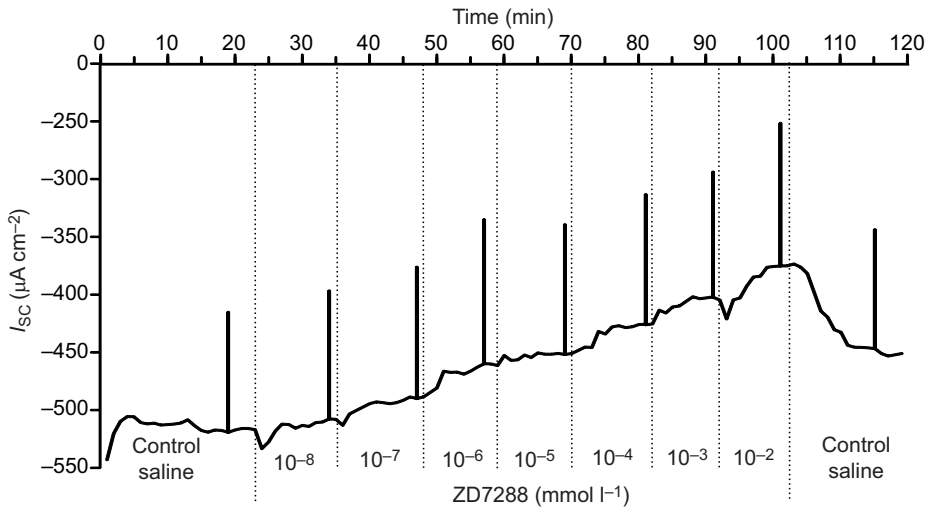

Fig. 6. Representative time course for the changes of I_{SC} across split lamellae of posterior gill 7 of *Carcinus maenas* applying basolateral ZD7288. I_{SC} is corrected for the fluid resistance, but not for the general decrease over time (see Materials and methods for details). The vertical current deflections reflect the conductance as assessed by the application of 5 mV voltage pulses.

Journal of Experimental Biology (2016) 219, 887-896 doi:10.1242/jeb.134502

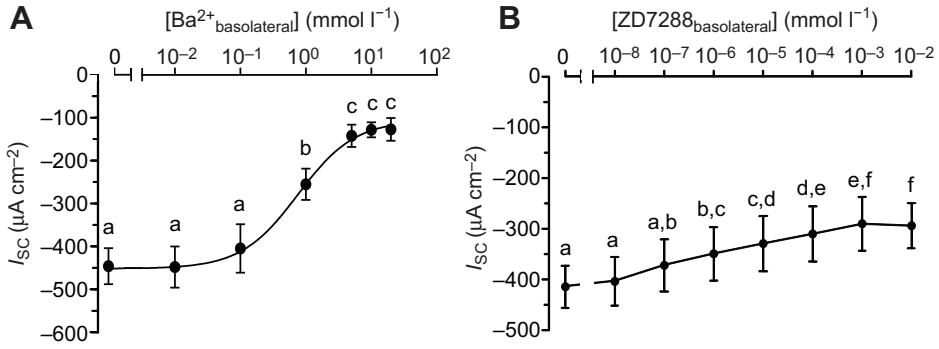

Fig. 7. Dose–response curves of potassium channel inhibitors with respect to I_{SC} in Ussing chamber experiments on split gill lamellae of *Carcinus maenas*. (A) Ba^{2+}; (B) ZD7288. All experiments were performed on split gill lamellae of posterior gill 7 of brackish-water-acclimated green crabs (11 ppt) under symmetrical conditions. IC_{50} for BaCl=0.76 mmol l^{-1}; IC_{50} for ZD7288=6×10^{-7} mmol l^{-1}. Different letters indicate significant differences in I_{SC} (repeated-measures ANOVA with Tukey's *post hoc* comparisons, $P<0.05$; $N_{Ba^{2+}}$=5–8 from four different animals, N_{ZD7288}=11 from five different animals).

observed in the present study in response to a respiratory acidosis caused by exposure to hypercapnia (Fehsenfeld and Weihrauch, 2013). Even though HCN homologs have been cloned from several invertebrate species and their hyperpolarization-activated current characteristics have been observed to closely resemble mammalian HCNs (Biel et al., 2009), their potential function has so far only been associated with chemo-sensitivity in the fruit fly *Drosophila melanogaster* (Chen and Wang, 2012) and signal transduction in olfactory neurons of the spiny lobster *Panulirus argus* (Gisselmann et al., 2005).

Therefore, the present study is the first to deliver evidence for a function of a conserved (ancestral) HCN as a key player in acid-base and ammonia regulation in an invertebrate.

Characterization of K^+-transport over the gill epithelium

Isolated gills

The results of the gill perfusion experiments clearly indicated at least two different K^+/NH_4^+-promoting structures in the branchial, basolateral epithelial membranes of *C. maenas*. These include at least one Ba^{2+}-sensitive K^+ channel, as well as the identified ZD7288-sensitive member of the hyperpolarization-activated cyclic nucleotide-gated K^+-channel family, CmHCN. The findings of the present study therefore strengthen results of earlier studies on split gill lamellae of *C. maenas* (Riestenpatt, 1995) and *E. sinensis* (Onken et al., 1991) that indicated that different populations of K^+ channels promote transcellular K^+ excretion because of the observed incomplete and complex di-phasic response of the I_{SC} when Ba^{2+} was applied to the apical and basolateral membranes, respectively.

Moreover, the participation of the respective K^+ channels in branchial acid-base and ammonia excretion became obvious by the observed decrease of ammonia and CO_2 excretion as well as the accumulation of protons in the perfusate with the basolaterally applied inhibitors Ba^{2+} and ZD7288 in posterior gill 7. Therefore, these results also support findings of a recent study that claim the ultimate linkage between acid-base and ammonia regulatory processes in the gill epithelium of this decapod crustacean by using the same transporter inventory (Fehsenfeld and Weihrauch, 2013). Interestingly, HCO_3^- excretion by the posterior gill is induced by ZD7288 but decreased with Ba^{2+}, thus verifying that the observed differences in excretion rates of ammonia, acid equivalents and CO_2 are not solely based on differences in the effective concentration of each inhibitor, but by the inhibitors targeting different K^+/NH_4^+-promoting structures.

Both inhibitors in the present study were applied basolaterally based on the fact that: (1) apical CsCl (10 mmol l^{-1}) had been shown to have no substantial effect on ammonia excretion in *C. maenas* (Weihrauch et al., 1998) even though it significantly reduced I_{SC} (Riestenpatt et al., 1996), and (2) the novel candidate gene CmHCN seemed to resemble the HCN2 as identified in basolateral membranes of the vertebrate kidney (Carrisoza-Gaytán et al., 2011) as discussed above. In the case of ZD7288, however, it cannot be excluded that it targeted the respective structure also in the apical membrane because of its strong lipophilic character and subsequent diffusion into the cell (Gasparini and DiFrancesco, 1997; Harris and Constanti, 1995). A predominantly intracellular presence and action of ZD7288 would also explain why the effect of this inhibitor as observed in gill perfusion experiments was not reversed in the wash step.

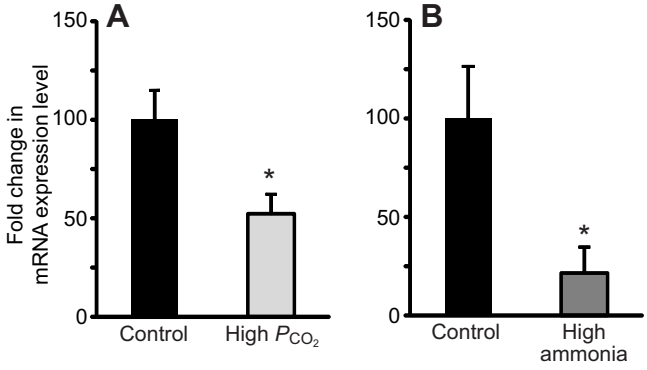

Fig. 8. mRNA expression changes of CmHCN in posterior gill 7 of brackish-water-acclimated *Carcinus maenas* (11 ppt) exposed to environmental stressors. (A) The light grey bar represents acclimation to high environmental P_{CO_2} (hypercapnia, 400 Pa, 7 days, N=6). mRNA expression for high P_{CO_2} acclimated animals was normalized to the ribosomal gene RbS-3 prior to calculation of relative gene expression changes. (B) The dark grey bar represents acclimation to high environmental ammonia (HEA, 1 mmol l^{-1} NH_4Cl, 7 days; N=4). Changes in mRNA levels in HEA acclimated animals were evaluated applying a standard curve (see Materials and methods for details). Values are given as means±s.e.m. Asterisks denote significant differences compared with control gene expression (Student's t-test, $P<0.05$).

Split gill lamellae

Further characterization of the effect of both inhibitors on overall epithelial ion movements and the resulting trans-epithelial current was achieved in Ussing chamber experiments on split gill lamellae. The observed values for general characteristics of split gill 7 were comparable to values in the literature. Even though slightly higher

Journal of Experimental Biology (2016) 219, 887-896 doi:10.1242/jeb.134502

outside positive potential differences were measured in posterior gill 7 in green crabs acclimated to 10 ppt in gill perfusion experiments (7.6±0.2 mV; Siebers et al., 1985), split gills seemed to generate a slightly lower potential difference of 6.6±1.3 mV (Onken and Siebers, 1992), which is even more comparable to the value observed in the present preparation (4.4±0.4 mV). Posterior gills of 10 ppt-acclimated *C. maenas* were also observed to generate an inward negative I_{SC} between −240 and −375 mA cm^{-2}, as well as a conductance of 40–45 mS cm^{-2} (Onken and Siebers, 1992; Riestenpatt et al., 1996), values that were also reached in the present study, validating the used technique.

The application of the inhibitors revealed the very different sensitivity of potential K^+ channels to Ba^{2+} and ZD7288. Under symmetrical conditions, the inward negative I_{SC} generated by the split gill epithelium of *C. maenas* is mainly carried by an electrogenic inward-directed Cl^- current dependent on the negative membrane potential over the basolateral membrane that is generated by the basolateral Na^+/K^+-ATPase and basolateral and apical K^+ channels (Riestenpatt et al., 1996). Increasing extracellular Cl^- concentrations by the addition of $BaCl_2$ would lead to the weakening of the driving force for Cl^- uptake and hence result in a passive decrease of I_{SC}. Hence, when not corrected for by addition of an equivalent concentration of Cl^- in the apical bath, no saturation of the effect of $BaCl_2$ on the I_{SC} was observed, and eventually, I_{SC} switched to inward positive values (>20 mmol l^{-1} $BaCl_2$, data not shown). Consequently, in the present study, preceding every increase in basolateral $BaCl_2$ concentration, choline chloride was added to the external bath to correct for this effect. As could be expected by an increased apical [Cl^-], I_{SC} became transitionally more negative. As a result, however, the effect of Ba^{2+} on the I_{SC} followed distinct Michaelis–Menten kinetics and the unbiased IC_{50} could be determined.

The IC_{50} for Ba^{2+} (0.76 mmol l^{-1}) in the split gill lamellae of green crab as determined in the present study was very similar to what was observed in the basolateral midgut epithelium of the tobacco hornworm, *Manduca sexta* (0.50 mmol l^{-1}; Zeiske et al., 1986), as well as the apical epithelium of frog skin (0.11 mmol l^{-1}; De Wolf and Van Driessche, 1986) and the basolateral epithelium of toad urinary bladder (1 mmol l^{-1}; Van Driessche and Erlij, 1988). At these relatively high concentrations, however, Ba^{2+} is believed to target delayed rectifier K^+ channels and K_V channels rather than K_{IR} and K_{Ca} channels (Rudy, 1988; Franchini et al., 2004). Hence, the obtained results are not conclusive in regard to the nature of the affected K^+ channel(s), taking into account that potentially all of the identified K^+ channels (K_V, K_{2P}, K_{Ca}, K_{IR} and HCN) might be present in the branchial epithelium and targeted by Ba^{2+}. At the concentration of 100 µmol l^{-1} that can still be considered specific for K_{IR} and K_{Ca} channels (Franchini et al., 2004; Hassinen et al., 2015), the observed inhibition of I_{SC} in the posterior gill 7 of osmoregulating *C. maenas* accounted for ca. 10% of the initial I_{SC}, indicating that a potential involvement of branchial K_{IR} and/or K_{Ca} channels cannot be excluded, but if present, only accounts for a minor fraction of the K^+ current. Furthermore, it cannot be excluded that Ba^{2+} also targets the HCN, as has been observed for high millimolar concentrations in the rat kidney (Carrisoza-Gaytán et al., 2011). According to the results of the present study, however, only ca. 30% of the measured K^+-related current can be assigned to the identified CmHCN in the branchial gill epithelium as demonstrated by the application of ZD7288. Consequently, the maximum observed effect of Ba^{2+} (73% inhibition of I_{SC}) remains partly unexplained for and additional experiments are necessary to further characterize the Ba^{2+}-sensitivity of the K^+ current in the branchial epithelium of *C. maenas*.

In contrast to the high effective concentration of Ba^{2+}, the unusually low IC_{50} of ZD7288 is astonishing. To verify the effect of ZD7288 and exclude a simply time-dependent shift of the I_{SC}, the dose–response curve has been corrected for the maximal time-dependent shift observed in split gill preparations without the application of inhibitors. Hence, the analysis represents a conservative approach and the observed effect of 30% inhibition on the I_{SC} might slightly underestimate the actual inhibition (ca. 5%). The IC_{50} for ZD7288 of 6×10^{-7} mmol l^{-1} in the present study is, to our knowledge, 500-fold smaller than the next smallest IC_{50} for ZD7288 determined in sinoatrial node cells isolated from the guinea pig heart (3×10^{-4} mmol l^{-1}; BoSmith et al., 1993) and can be interpreted as an extremely high affinity of this reagent for CmHCN and/or a comparably low abundancy of the protein in the branchial epithelium. The fact that CmHCN mRNA expression levels in posterior gills of *C. maenas* are similarly high compared with those observed for the Na^+/K^+-ATPase (Fehsenfeld and Weihrauch, 2013) and a pronounced effect of 10 µmol l^{-1} was observed in isolated gills perfusion experiments, however, rather supports the high binding capacity of this inhibitor. Generally, similar to Ba^{2+}, the mode of action of ZD7288 is voltage-dependent and related to the ambient K^+ concentration (Cheng et al., 2007), and might therefore differ substantially from other tissues and organisms, explaining the observed differences in IC_{50} values for ZD7288, but also for Ba^{2+}.

Furthermore, the potency of ZD7288 was shown to depend on the respective HCN isoform in mammalian tissues and blocked the I_F ('funny') current in the sinoatrial node more effectively ($IC_{50}=3\times10^{-4}$ mmol l^{-1}; BoSmith et al., 1993) than the I_h ('hyperpolarization'-activated) current in neurons ($IC_{50}=2$-41×10^{-3} mmol l^{-1}; Shin et al., 2001). Hence, even though highly conserved on the protein level, the potentially single HCN in *C. maenas* might exhibit different features regarding ZD7288 binding that make it more sensitive for the block [i.e. shifts in hydrophobicity (Cheng et al., 2007) and epigenetic factors altering methyl-dependent polarization, as observed for Ba^{2+} (Rossi et al., 2013)].

Even though the present study clearly showed that the involvement of HCN in branchial K^+/NH_4^+ transport accounted for ca. 30% of the K^+-generated current, the full extent of the Ba^{2+}-related block cannot be explained at this point. The analysis of the *C. maenas* transcriptome and subsequent gene tree analysis revealed a potential role for all major classes of K^+ channels in the generation of (branchial) K^+ currents in the green crab. After verifying the mRNA and/or protein expression pattern for each of the newly identified candidate genes in the green crab, further research also needs to be done to fully characterize the K^+ current in the branchial epithelium.

Conclusions

In conclusion, the present study strongly indicates the involvement of a basolateral HCN-like potassium channel in branchial acid-base and ammonia regulation in the decapod crustacean *C. maenas*. Besides potential other basolateral Ba^{2+}-sensitive K^+ channel(s), gill perfusion experiments applying the HCN-specific inhibitor ZD7288 show that this novel candidate gene is involved in NH_4^+ transport over the basolateral gill epithelial membrane. Interestingly, similar features (i.e. the potential dual transport capabilities of K^+ and NH_4^+ and decreased mRNA expression changes in response to metabolic acidosis) have been observed for the HCN2 expressed in the mammalian kidney, indicating a conserved function of this gene for basic homeostatic regulation throughout the animal kingdom. The high level of conservation of the amino acid sequence between invertebrate and vertebrate HCNs strengthens the importance of this

gene as a potential key player in acid-base and ammonia regulation in vertebrates as well as invertebrates. However, as this only accounts for ca. 30% of the K^+-related trans-epithelial short-circuit current, further research should be carried out to elucidate the nature of the complete K^+-dependent current in the gill epithelium of *C. maenas*.

Acknowledgements
The authors thank Drs Greg G. Goss, Chris M. Wood and Tamzin Blewett, as well as the staff of the Bamfield Marine Sciences Center, for the help in collecting the green crabs. Additional thanks go to the Animal Holding Facility of the University of Manitoba for taking care of the crabs. Thanks go also to Dr Frank Melzner for providing supervision, space and laboratory equipment for gill perfusion experiments on *C. maenas* in Kiel, Germany, and to Michael Gaudry, who assisted with the transcriptome analysis.

Competing interests
The authors declare no competing or financial interests.

Author contributions
S.F. performed all experiments and all data analyses as part of her PhD thesis. D.W. helped with the design of the study, edited the manuscript and provided financial support, as well as laboratory equipment in Winnipeg, Canada.

Funding
This work was funded by a NSERC Discovery Grant (D.W.) and a University of Manitoba Graduate Fellowship (S.F.), as well as a student travel and research grant of the Faculty of Graduate Studies/Faculty of Science/Department of Biology of the University of Manitoba (S.F.).

References
Biel, M., Wahl-Schott, C., Michalakis, S. and Zong, X. (2009). Hyperpolarization-activated cation channels: from genes to function. *Physiol. Rev.* **89**, 847-885.
BoSmith, R. E., Briggs, I. and Sturgess, N. C. (1993). Inhibitory actions of ZENECA ZD7288 on whole-cell hyperpolarization activated inward current (I_f) in guinea-pig dissociated sinoatrial node cells. *Br. J. Pharmacol.* **110**, 343-349.
Carrisoza-Gaytán, R., Rangel, C., Salvador, C., Saldaña-Meyer, R., Escalona, C., Satlin, L. M., Liu, W., Zavilowitz, B., Trujillo, J., Bobadilla, N. A. et al. (2011). The hyperpolarization-activated cyclic nucleotide-gated HCN2 channel transports ammonium in the distal nephron. *Kidney Int.* **80**, 832-840.
Chen, Z. J. and Wang, Z. R. (2012). Functional study of hyperpolarization activated channel (I_h) in *Drosophila* behavior. *Sci. China Life Sci.* **55**, 2-7.
Cheng, L., Kinard, K., Rajamani, R. and Sanguinetti, M. C. (2007). Molecular mapping of the binding site for a blocker of hyperpolarization-activated, cyclic nucleotide-modulated pacemaker channels. *J. Pharmacol. Exp. Ther.* **322**, 931-939.
Choe, S. (2002). Potassium channel structures. *Nat. Rev. Neurosci.* **3**, 115-121.
De Wolf, I. and Van Driessche, W. (1986). Voltage-dependent Ba^{2+} block of K^+ channels in apical membrane of frog skin. *Am. J. Physiol.* **251**, C696-C706.
DiFrancesco, D. (1993). Pacemaker mechanisms in cardiac tissue. *Annu. Rev. Physiol.* **55**, 455-472.
Fehsenfeld, S. and Weihrauch, D. (2013). Differential acid-base regulation in various gills of the green crab *Carcinus maenas*: effects of elevated environmental pCO_2. *Comp. Biochem. Physiol. A* **164**, 54-65.
Franchini, L., Levi, G. and Visentin, S. (2004). Inwardly rectifying K^+ channels influence Ca^{2+} entry due to nucleotide receptor activation in microglia. *Cell Calcium* **35**, 449-459.
Gasparini, S. and DiFrancesco, D. (1997). Action of the hyperpolarization-activated current (I_h) blocker ZD 7288 in hippocampal CA1 neurons. *Pflügers Arch. Eur. J. Physiol.* **435**, 99-106.
Gisselmann, G., Marx, T., Bobkov, Y., Wetzel, C. H., Neuhaus, E. M., Ache, B. W. and Hatt, H. (2005). Molecular and functional characterization of an I_h-channel from lobster olfactory receptor neurons. *Eur. J. Neurosci.* **21**, 1635-1647.
Hammer, Ø., Harper, D. A. T. and Ryan, P. D. (2001). PAST: paleontological statistics software package for education and data analysis. *Palaeontol. Electron* **4**, 9-18.
Harris, N. C. and Constanti, A. (1995). Mechanism of block by ZD 7288 of the hyperpolarization-activated inward rectifying current in guinea pig substantia nigra neurons *in vitro*. *J. Neurophysiol.* **74**, 2366-2378.
Hassinen, M., Haverinen, J., Hardy, M. E., Shiels, H. A. and Vornanen, M. (2015). Inward rectifier potassium current (I_{K1}) and Kir2 composition of the zebrafish (*Danio rerio*) heart. *Pflügers Arch.* **467**, 2437-2446. .
Hibino, H., Inanobe, A., Furutani, K., Murakami, S., Findlay, I. and Kurachi, Y. (2010). Inwardly rectifying potassium channels: their structure, function, and physiological roles. *Physiol. Rev.* **90**, 291-366.
Jones, D. T., Taylor, W. R. and Thornton, J. M. (1992). The rapid generation of mutation data matrices from protein sequences. *Comput. Appl. Biosci.* **8**, 275-282.
Larsen, E. H., Deaton, L. E., Onken, H., O'Donnell, M., Grosell, M., Dantzler, W. H. and Weihrauch, D. (2014). Osmoregulation and excretion. *Compr. Physiol.* **4**, 405-573.
Le, S. Q. and Gascuel, O. (2008). An improved general amino acid replacement matrix. *Mol. Biol. Evol.* **25**, 1307-1320.
Lignon, J. M. (1987). Ionic permeabilities of the isolated gill cuticle of the shore crab *Carcinus maenas*. *J. Exp. Biol.* **131**, 159-174.
Onken, H. and Siebers, D. (1992). Voltage-clamp measurements on single split lamellae of posterior gills of the shore crab *Carcinus maenas*. *Mar. Biol.* **114**, 385-390.
Onken, H., Graszynski, K. and Zeiske, W. (1991). Na^+-independent, electrogenic Cl^- uptake across the posterior gills of the Chinese crab (*Eriocheir sinensis*): voltage-clamp and microelectrode studies. *J. Comp. Physiol. B* **161**, 293-301.
Onken, H., Tresguerres, M. and Luquet, C. M. (2003). Active NaCl absorption across posterior gills of hyperosmoregulating *Chasmagnathus granulatus*. *J. Exp. Biol.* **206**, 1017-1023.
Riestenpatt, S. (1995). *Die osmoregulatorische NaCl-Aufnahme über die Kiemen decapoder Crustaceen (Crustacea, Decapoda)*. Berlin: VWF Verlag für Wissenschaft und Forschung.
Riestenpatt, S., Onken, H. and Siebers, D. (1996). Active absorption of Na^+ and Cl^- across the gill epithelium of the shore crab *Carcinus maenas*: voltage-clamp and ion-flux studies. *J. Exp. Biol.* **199**, 1545-1554.
Rossi, M., Tkatchenko, A., Rempe, S. B. and Varma, S. (2013). Role of methyl-induced polarization in ion binding. *Proc. Natl. Acad. Sci. USA* **110**, 12978-12983.
Rudy, B. (1988). Diversity and ubiquity of K channels. *Neuroscience* **25**, 729-749.
Schirmanns, K. and Zeiske, W. (1994). An investigation of the midgut K^+ pump of the tobacco hornworm (*Manduca sexta*) using specific inhibitors and amphotericin B. *J. Exp. Biol.* **188**, 191-204.
Schwarz, H.-J. and Graszynski, K. (1989). Ion transport in crab gills: a new method using isolated half platelets of *Eriocheir* gills in an ussing-type chamber. *Comp. Biochem. Physiol. A* **92**, 601-604.
Shin, K. S., Rothberg, B. S. and Yellen, G. (2001). Blocker state dependence and trapping in hyperpolarization-activated cation channels: evidence for an intracellular activation gate. *J. Gen. Physiol.* **117**, 91-102.
Siebers, D., Winkler, A., Lucu, C., Thedens, G. and Weichart, D. (1985). Na-K-ATPase generates an active transport potential in the gills of the hyperregulating shore crab *Carcinus maenas*. *Mar. Biol.* **87**, 185-192.
Skou, J. C. (1960). Further investigations on a Mg^{++}+Na^+-activated adenosinetriphosphatase, possible related to the active, linked transport of Na^+ and K^+ across the nerve membrane. *Biochim. Biophys. Acta* **42**, 6-23.
Tamura, K., Stecher, G., Peterson, D., Filipski, A. and Kumar, S. (2013). MEGA6: Molecular evolutionary genetics analysis version 6.0. *Mol. Biol. Evol.* **30**, 2725-2729.
Tian, C., Zhu, R., Zhu, L., Qiu, T., Cao, Z. and Kang, T. (2014). Potassium channels: structures, diseases, and modulators. *Chem. Biol. Drug Des.* **83**, 1-26.
Truchot, J.-P. (1976). Carbon dioxide combining properties of the blood of the shore crab *Carcinus maenas* (L.): carbon dioxide solubility coefficient and carbonic acid dissociation constants. *J. Exp. Biol.* **64**, 45-57.
Van Driessche, W. and Erlij, D. (1988). Activation of K^+ conductance in basolateral membrane of toad urinary bladder by oxytocin and cAMP. *Am. J. Physiol.* **254**, C816-C821.
Verbruggen, B., Bickley, L. K., Santos, E. M., Tyler, C. R., Stentiford, G. D., Bateman, K. S. and van Aerle, R. (2015). De novo assembly of the *Carcinus maenas* transcriptome and characterization of innate immune system pathways. *BMC Genomics* **16**, 458.
Weihrauch, D., Becker, W., Postel, U., Riestenpatt, S. and Siebers, D. (1998). Active excretion of ammonia across the gills of the shore crab *Carcinus maenas* and its relation to osmoregulatory ion uptake. *Comp. Biochem. Physiol. B* **168**, 364-376.
Weihrauch, D., Becker, W., Postel, U., Luck-Kopp, S. and Siebers, D. (1999). Potential of active excretion of ammonia in three different haline species of crabs. *J. Comp. Physiol. B* **169**, 25-37.
Weiner, I. D. and Verlander, J. W. (2013). Renal ammonia metabolism and transport. *Comp. Physiol.* **3**, 201-220.
Wollmuth, L. P. (1994). Mechanism of Ba^{2+} block of M-like K channels of rod photoreceptors of tiger salamanders. *J. Gen. Physiol.* **103**, 45-66.
Zeiske, W., Van Driessche, W. and Ziegler, R. (1986). Current-noise analysis of the basolateral route for K^+-ions across a K^+-secreting insect midgut epithelium. *Pflügers Arch. Eur. J. Physiol.* **407**, 657-663.